Dalton Transactions

Accepted Manuscript

ROYAL SOCIETY OF CHEMISTRY

www.rsc.org/dalton

Journal Name

RSCPublishing

ARTICLE

Synthesis and structural analyses of phenylethynyl-substituted tris(2-pyridylmethyl)amines and their copper(II) complexes†

Cite this: DOI: 10.1039/xoxxoooooox

Received ooth January 2012,
Accepted ooth January 2012

DOI: 10.1039/xoxxoooooox

www.rsc.org/

Jaebum Lim,[ab] Vincent M. Lynch,[a] Ramakrishna Edupuganti,[a] Andrew Ellington*[b] and Eric V. Anslyn*[a]

Three new tris(2-pyridylmethyl)amine-based ligands possessing phenylethynyl units have been prepared using Sonogashira couplings and substitution reactions. Copper(II) complexes of those tetradentate ligands have also been synthesized. Solid-state structures of the six new compounds have been determined by single-crystal X-ray diffraction analyses. Examination of the molecular structures of the ligands revealed the expected triangular geometries with virtually undeformed carbon-carbon triple bonds. While the tertiary nitrogen of the free ligands seem to be prevented from participation in supramolecular non-covalent interactions by the pyridyl hydrogen at the 3-position, the pyridyl nitrogens play a crucial role in the packing mode of the crystal structure. The nitrogens form weak hydrogen bonds, varied in length between 2.32 and 2.66 Å, with the pyridyl hydrogen of its neighbouring molecule. The [N···H–C] contacts enforce one-dimensional columnar assemblies on ligands that organize into wall-like structures, which in turn assemble into three-dimensional structures through CH–π interactions. Structural analyses of Cu(II) complexes of the ligands revealed propeller-like structures caused by steric crowding of three pyridine ligands. The copper complexes of the ligands having three phenylethynyl substituents showed a remarkably deformed carbon-carbon triple bond enforced by a steric effect of the three phenyl groups. Most significantly, a total of seventy non-covalent interactions, classified into twelve types of hydrogen-involved short contacts, were identified in this study. The phenylethynyl substituent participated in forty-two interactions as a hydrogen bond acceptor, and its role was more distinctive in the crystal structures of the Cu(II) complexes.

Introduction

Tris(2-pyridylmethyl)amine (TPMA; or tris(2-picolyl)amine, TPA) is neutral ligand that has four binding sites—three pyridyl nitrogens and a central amine nitrogen—with a tripodal structure. TPMA can bind to a multitude of transition metals[1–8] including lanthanides and actinides,[9–13] as well as most alkali and alkali earth metals[14–16] due to its excellent chelating ability to a metal in a tridentate or a tetradentate manner. Thus, TPMA has been used as an indispensable ligand in many transition-metal mediated organic reactions, such as iron-catalyzed olefin oxidations,[17,18] copper-catalyzed azide-alkyne cycloadditions,[19] and copper-catalyzed atom transfer radical polymerization (ATRP) reactions.[20,21]

Modified TPMA ligands that preserve the tripodal structure and the strong metal-binding affinity have received considerable attention as ligands and/or hosts for molecular recognition purposes. Because of steric crowding of three pyridine ligands, a TPMA-metal complex has a propeller-like structure where all three rings are twisted in the same direction, with a right- or left-handed helix. Canary and co-workers have studied metal complexes of chiral TPMA derivatives with Cu^{2+}, Zn^{2+}, and Cd^{2+} for the purpose of identification of absolute configuration.[22–27] Previous work from our group has focused on the use of TPMA derivatives and their metal complexes as sensors for chiral amino acids[28,29] and chiral secondary alcohols,[30–35] as well as hosts for phosphate recognition.[36–38]

Because of their pro-axial chirality and a wide range of use, TPMA and its structural relatives are promising chelators for organometallic materials such as catalysts and chirality sensors. In the process of creating sensors for determining the handedness of various chiral functional groups acting as metal ligands, we generated a series of new TPMA ligands. We found that these ligands were extremely crystalline, both in their free and metalated forms. From this perspective, the structural diversification of the TPMA ligand led to a study of

crystalline packing forces, and numerous interactions of various sorts were revealed. Here, we present the synthesis of new TPMA derivatives **1**–**3,** and their Cu^{2+} complexes **4**–**6**, along with a detailed analysis of their solid-state structures.

Experimental section

General procedures

Scheme 1 Synthesis of Compound **1–6**

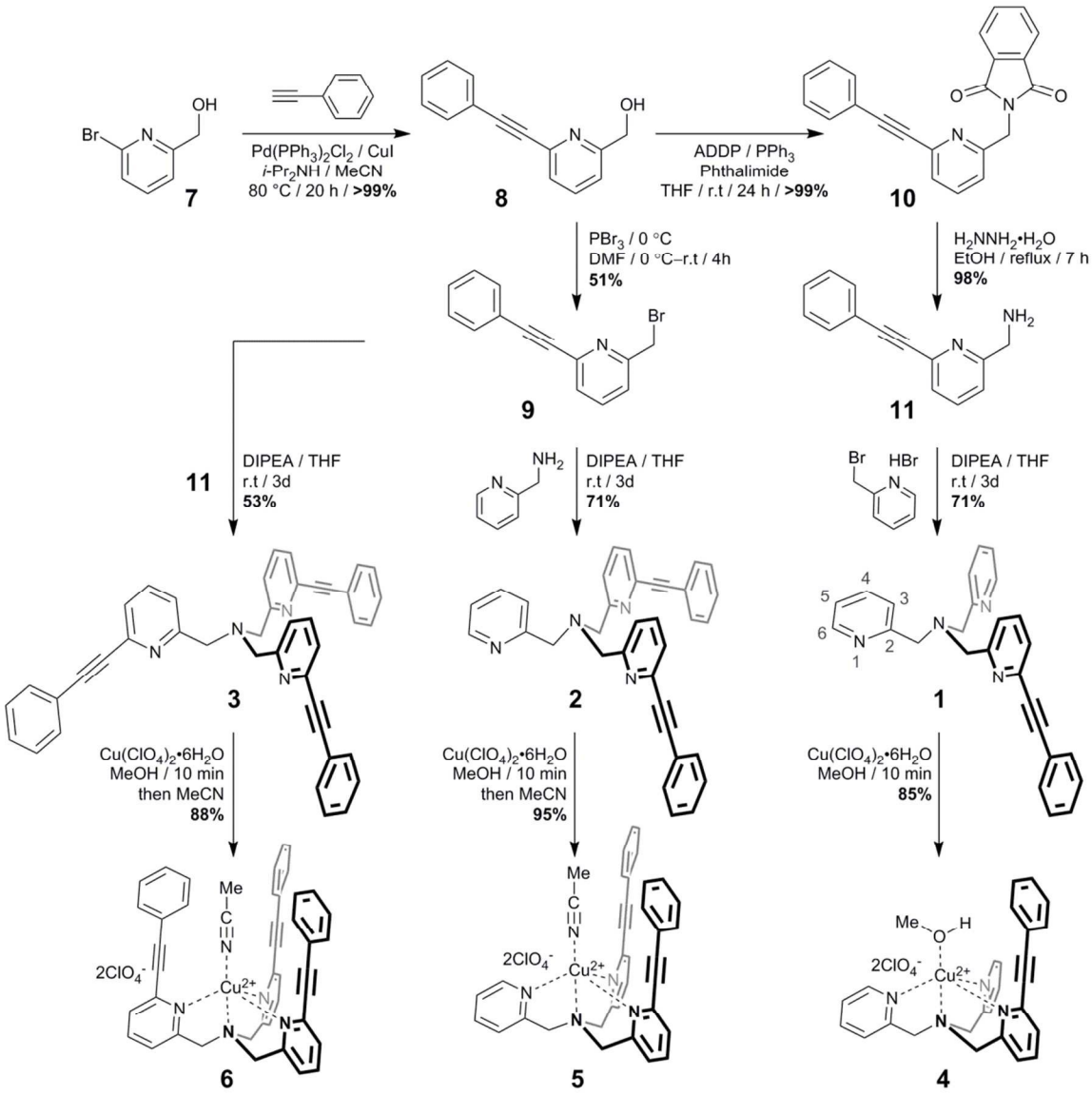

All reactions were performed under nitrogen in flame-dried glassware. Reagents and solvents were purchased from commercial suppliers and used without further purification. *CAUTION! Copper(II)perchlorate is potentially explosive and should be handled with care.* Diisopropylamine was distilled over KOH pellets and degassed by a 15 min nitrogen purge prior to use. Column chromatography was carried out on silica gel with particle size 40–63 μm (230×400 mesh). Analytical TLC was performed on Merck silica-gel glass plates. Melting points were performed in open capillary tubes, using a Stanford Research Systems MPA 100 OptiMelt automated melting point apparatus. NMR spectra were recorded on a VARIAN DirectDrive 400 MHz spectrometer. All ^{13}C-NMR spectra were recorded with simultaneous decoupling of ^{1}H nuclei. The chemical shifts of ^{1}H NMR and ^{13}C NMR are reported in ppm units relative to the residual signal of $CDCl_3$ solvent (7.26 ppm for ^{1}H and 77.16 ppm for ^{13}C). All NMR spectra were recorded at 25 °C. High resolution mass spectra (HRMS) were obtained on an Agilent 6530 QTOF (ESI) mass spectrometer by the Mass Spectrometry Facility of the Department of Chemistry at the University of Texas at Austin.

Syntheses of materials

Compound 8. Phenylacetylene (3.26 g, 31.9 mmol) was added to a 250 mL round-bottom flask equipped with a Friedrich condenser containing the mixture of 2-bromo-6-(hydroxymethyl)pyridine **7** (3.00 g, 16.0 mmol),[39] $PdCl_2(PPh_3)_2$ (280 mg, 0.399 mmol),[40] CuI (76.0 mg, 0.399 mmol), *i*-Pr_2NH

(50 mL), and MeCN (50 mL). The mixture was stirred for 20 hours at 80 °C. After cooling, the solvent was removed under reduced pressure, and the crude mixture purified by column chromatography, eluting with hexanes/ethyl acetate mixtures in 4:1, 2:1, and 1:1 ratios. The eluent was evaporated to give dark-brown oil as a product in 99% yield (3.30 g, 15.9 mmol). ^{1}H NMR ($CDCl_3$, 400 MHz): δ 7.69 (t, $^3J_{H–H}$= 7.8 Hz, 1H), 7.61 (m, 2H), 7.45 (d, $^3J_{H–H}$= 7.8 Hz, 1H), 7.38 (m, 3H), 7.24 (d, $^3J_{H–H}$= 7.8 Hz, 1H), 4.79 (d, $^3J_{H–H}$= 5.1 Hz, 2H), 3.48 (t, $^3J_{H–H}$= 5.1 Hz, 1H). ^{13}C NMR ($CDCl_3$, 100 MHz): δ 160.16, 142.34, 136.97, 132.11, 129.15, 128.49, 125.97, 122.16, 119.88, 89.64, 88.46, 64.53. HRMS (ESI/[M+H]$_+$) calcd. for $C_{14}H_{11}NO$: 210.0913. Found: 210.0912.

Compound 9.[41] Compound **8** (1.50 g, 7.17 mmol) was dissolved in 5 mL of DMF. The 25 mL round-bottom flask was immersed in an ice bath and vigorously stirred. PBr_3 (2.33 g, 8.60 mmol) was slowly added dropwise via syringe. After the color of the reaction mixture turned black, the ice bath was removed, and the solution was stirred for 4 hours at room temperature (20 °C). Water (5 mL) was slowly added, and the mixture was diluted with 30 mL of Et_2O. The whole mixture was washed with water (20 mL × 3), dried over Na_2SO_4, filtered and evaporated to dryness. The solid residue was purified by column chromatography, eluting with hexanes and hexanes/ethyl acetate mixtures in 8:1 and 4:1 ratios. The solvent was removed by using a rotavaporator to afford compound **9** as a brownish solid in 51% yield (1.00 g, 3.67 mmol). Compound **9** decomposed at 166 °C. ^{1}H NMR ($CDCl_3$, 400 MHz): δ 7.70 (t, $^3J_{H–H}$= 7.8 Hz, 1H), 7.61 (m, 2H), 7.46 (d, $^3J_{H–H}$= 7.8 Hz, 1H), 7.43 (d, $^3J_{H–H}$= 7.8 Hz, 1H), 7.36 (m, 3H), 4.57 (s, 2H). ^{13}C NMR ($CDCl_3$, 100 MHz): δ 157.40, 143.14, 137.46, 132.21, 129.24, 128.49, 126.65, 122.88, 122.12, 89.92, 88.25, 33.50. HRMS (ESI/[M+H]$^+$) calcd. for $C_{14}H_{10}BrN$: 272.0069. Found: 272.0071.

Compound 10.[42] To a 100 mL round-bottom flask containing a THF (50 mL) solution of compound **8** (1.15 g, 5.51 mmol) was added 1,1'-(azodicarbonyl)dipiperidine (ADDP, 1.81 g, 7.16 mmol). The mixture was stirred for 2 minutes at room temperature (20 °C), then PPh_3 (1.88 g, 7.16 mmol) and phthalimide (1.05 g, 7.16 mmol). The reaction mixture was stirred for 24 hours at room temperature, and cooled to 0 °C. A solid precipitate formed, filtrated on a Buchner filter, and washed with cold THF (50 mL × 2). The filtrate was concentrated on a rotavaporator and diluted with a saturated aqueous solution of $NaHCO_3$ (150 mL). Organic compounds in the mixture were extracted with ethyl acetate (100 mL × 2), and the combined organic layer was dried over anhydrous Na_2SO_4, and filtered over a Buchner funnel. The solvent was removed, and the residue was purified by column chromatography, eluting with hexanes/ethyl acetate mixtures in 4:1, 2:1, and 1:1 ratios. The isolated pure product was concentrated to dryness in vacuo to give a white solid in 99% yield (1.85 g, 5.47 mmol). ^{1}H NMR ($CDCl_3$, 400 MHz): δ 7.91 (dd, $^3J_{H–H}$= 5.5 Hz, $^3J_{H–H}$= 3.1 Hz, 2H), 7.76 (dd, $^3J_{H–H}$= 5.5 Hz, $^3J_{H–H}$= 3.1 Hz, 2H), 7.62 (t, $^3J_{H–H}$= 7.8 Hz, 1H), 7.58 (m, 2H), 7.42 (d, $^3J_{H–H}$= 7.8 Hz, 1H), 7.35 (m, 3H), 7.14 (d, $^3J_{H–H}$= 7.8 Hz, 1H), 5.06 (s, 2H). ^{13}C NMR ($CDCl_3$, 100 MHz): δ 168.08, 156.24, 143.28, 137.04, 134.26, 132.19, 132.15, 129.06, 128.43, 126.25, 123.65, 122.29, 120.14, 89.54, 88.67, 43.22. HRMS (ESI/[M+H]$^+$) calcd. for $C_{22}H_{14}N_2O_2$: 339.1128. Found: 339.1131.

Compound 11.[42] A round-bottom flask (100 mL) was charged with a suspension of compound **10** (1.24 g, 3.66 mmol) in 40 mL of absolute ethanol, and equipped with a Friedrich condenser. The suspension was heated to reflux until complete dissolution. Hydrazine monohydrate (734 mg, 14.7 mmol) was added to the solution. The color of the reaction mixture turned yellow within a minute, and a solid by-product was observed in 3 hours of heating. The mixture was diluted with an additional 20 mL of ethanol and stirred for an extra 2 hours. After cooling, an oil bath was replaced with an ice bath to further precipitate

Table 1 Crystallographic data for compound **1–6**

Compound reference	**1**	**2**	**3**	**4**	**5**	**6**
Chemical formula	$C_{26}H_{22}N_4$	$C_{34}H_{26}N_4$	$C_{42.5}H_{31}ClN_4$ [a]	$C_{27}H_{26}Cl_2CuN_4O_9$	$C_{36}H_{29}Cl_2CuN_5O_8$	$C_{44}H_{33}Cl_2CuN_5O_8$
Formula Mass	390.47	490.59	633.16 [a]	684.96	794.08	894.19
Crystal system	Monoclinic	Triclinic	Monoclinic	Monoclinic	Triclinic	Triclinic
a/Å	23.3542(19)	6.1075(12)	37.576(3)	10.9021(8)	11.6528(11)	12.7070(14)
b/Å	6.1583(6)	18.770(3)	6.0193(4)	22.0571(19)	12.4257(13)	13.1550(15)
c/Å	29.500(3)	24.794(4)	30.017(2)	12.5252(8)	13.8814(15)	14.596(2)
α/°	90	108.838(6)	90	90	99.698(3)	116.759(3)
β/°	94.130(6)	90.297(6)	106.952(2)	106.189(8)	111.246(3)	107.160(3)
γ/°	90	98.256(6)	90	90	100.405(2)	90.037(4)
Unit cell volume/Å^3	4231.8(6)	2658.2(8)	6494.2(8)	2892.5(4)	1781.5(3)	2056.0(4)
Temperature/K	133(2)	133(2)	100(2)	150(2)	100(2)	143(2)
Space group	*C* 2/c	*P*$\bar{1}$	*C* 2/c	*P* 2$_1$/n	*P*$\bar{1}$	*P*$\bar{1}$
No. of formula units per unit cell, *Z*	8	4	8	4	2	2
Radiation type	MoK$_\alpha$	MoK$_\alpha$	MoK$_\alpha$	MoK$_\alpha$	MoK$_\alpha$	MoK$_\alpha$
Absorption coefficient, μ/mm^{-1}	0.074	0.073	0.156	1.000	0.822	0.722
No. of reflections collected	42921	24454	37888	28259	37865	23144
No. of independent reflections	4834	9316	7387	6631	8127	5877
R_{int}	0.1208	0.1166	0.0767	0.0433	0.0635	0.0653
R_1 ($I > 2\sigma(I)$)	0.0641	0.0731	0.0793	0.0807	0.0351	0.0787
$wR(F^2)$ ($I > 2\sigma(I)$)	0.1486	0.1336	0.2015	0.2166	0.0916	0.1916
R_1 (all data)	0.1177	0.2020	0.1137	0.1061	0.0380	0.1118
$wR(F^2)$ (all data)	0.1906	0.1664	0.2212	0.2361	0.0934	0.2074
Goodness of fit on F^2	1.028	1.027	1.044	1.047	1.049	1.283
CCDC	1028486	1028487	1028485	1028490	1028488	1028489

[a] The contributions to the scattering factors due to disordered solvent molecules were removed by use of the utility SQUEEZE in PLATON98.

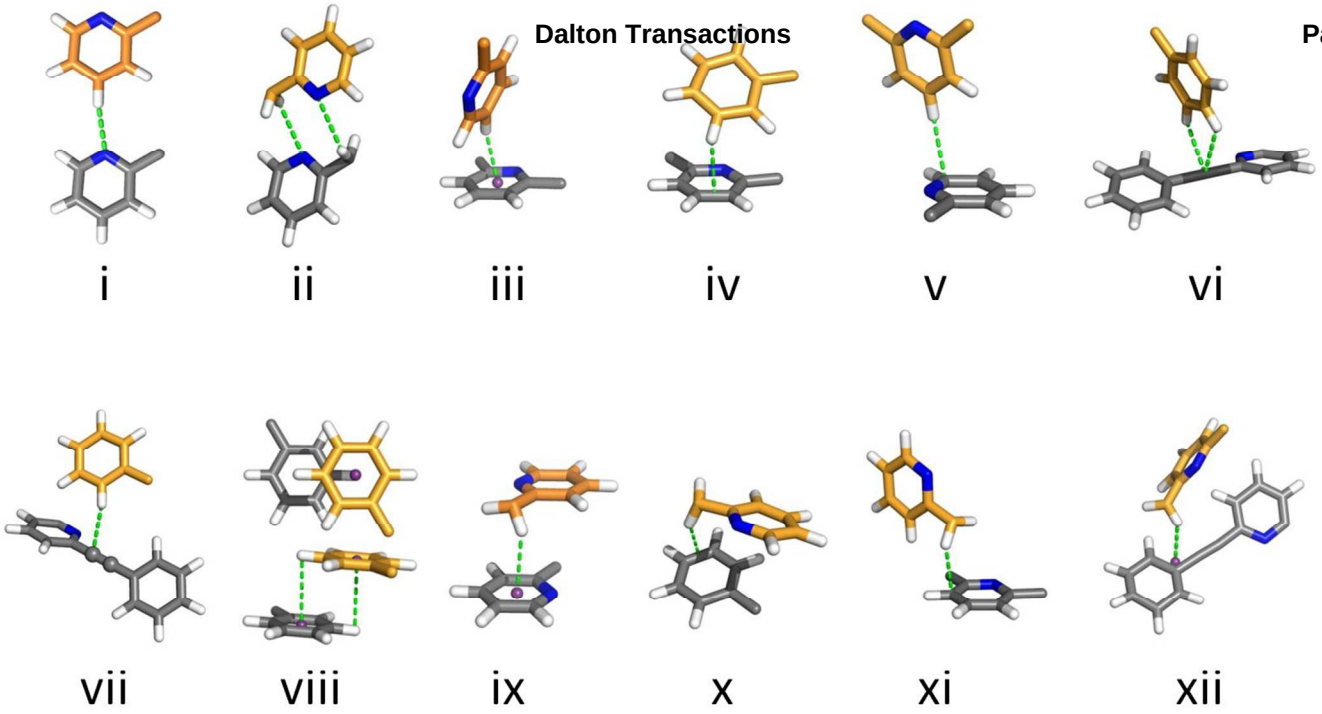

Fig. 1 Twelve types of non-covalent interactions that are found in X-ray crystal structures of compound 1–6. C—orange and gray, H—white, N—blue and centroid—violet purple.

the hydrazine-phthalimide byproduct. The precipitate was washed with cold absolute ethanol (100 mL) on a Buchner funnel, and the filtrate was concentrated. The sticky residue was diluted with cold ethanol, and filtered again to remove solids. The filtrate was concentrated again to dryness. The product (748 mg, 3.59 mmol, 98% yield) was clean by NMR, and used without further purification for the next step. ^{1}H NMR ($CDCl_3$, 400 MHz): δ 7.66 (t, $^{3}J_{H–H}$= 7.7 Hz, 1H), 7.61 (m, 2H), 7.42 (d, $^{3}J_{H–H}$= 7.7 Hz, 1H), 7.36 (m, 3H), 7.27 (d, $^{3}J_{H–H}$= 7.7 Hz, 1H), 4.00 (s, 2H). ^{13}C NMR ($CDCl_3$, 100 MHz): δ 142.94, 136.89, 132.13, 129.06, 128.45, 125.66, 122.45, 122.29, 120.68, 89.25, 88.74, 47.73. HRMS (ESI/[M+H]$^+$) calcd. for $C_{14}H_{12}N_2$: 209.1073. Found: 209.1072.

General method for compounds 1–3.[43] **Compound 1**. A 100 mL round-bottom flask was charged with diisopropylethylamine (DIPEA, 745 mg, 5.76 mmol), 2-(bromomethyl)pyridine hydrogen bromide (729 mg, 2.88 mmol), and 30 mL of THF. Compound **11** (300 mg, 1.44 mmol) in 10 mL of THF was added dropwise to the flask, and the mixture was stirred for 3 days at room temperature (20 °C). The mixture was concentrated in vacuo to dryness, and purified by column chromatography, eluting with CH_2Cl_2 and the mixture of MeOH/CH_2Cl_2 in 2:98, 5:95, and 10:90 ratios. The product fraction was collected, and the solvent was evaporated to give a white solid (mp 120 °C) in 71% yield (400 mg, 1.02 mmol). ^{1}H NMR ($CDCl_3$, 400 MHz): δ 8.54 (ddd, $^{3}J_{H–H}$= 4.9 Hz, $^{4}J_{H–H}$= 1.6 Hz, $^{5}J_{H–H}$= 0.8 Hz, 2H), 7.70–7.54 (m, 8H), 7.40 (dd, $^{3}J_{H–H}$= 7.3 Hz, $^{4}J_{H–H}$= 1.4 Hz, 1H), 7.35 (m, 3H), 7.15 (ddd, $^{3}J_{H–H}$= 7.4 Hz, $^{3}J_{H–H}$= 4.9 Hz, $^{4}J_{H–H}$= 1.2 Hz, 2H), 3.93 (s, 2H), 3.91 (s, 4H). ^{13}C NMR ($CDCl_3$, 100 MHz): δ 160.31, 159.31, 149.22, 142.64, 136.69, 136.50, 132.11, 128.95, 128.40, 125.75, 123.03, 122.39, 122.11, 122.02, 89.11, 88.83, 60.27, 60.21. HRMS (ESI/[M+H]$^+$) calcd. for $C_{26}H_{22}N_4$: 391.1917. Found: 391.1921.

Compound 2. A 50 mL round-bottom flask was charged with DIPEA (478 mg, 3.70 mmol), compound **9** (503 mg, 1.85 mmol), and 20 mL of THF. The solution of 2-(aminomethyl)pyridine (100 mg, 0.925 mmol) in 5 mL of THF was added dropwise to the flask, and the mixture was stirred for 3 days at room temperature (20 °C). The product of this reaction was afforded as a white solid (mp 142 °C) in 71% yield (321 mg, 0.654 mmol) with the general method described above. ^{1}H NMR ($CDCl_3$, 400 MHz): δ 8.53 (ddd, $^{3}J_{H–H}$= 4.9 Hz, $^{4}J_{H–H}$= 1.7 Hz, $^{5}J_{H–H}$= 0.8 Hz, 1H), 7.68–7.61 (m, 3H), 7.61–7.55 (m, 6H), 7.54 (d, $^{3}J_{H–H}$= 7.8 Hz, 1H), 7.38 (dd, $^{3}J_{H–H}$= 7.5 Hz, $^{4}J_{H–H}$= 1.2 Hz, 2H), 7.35–7.30 (m, 6H), 7.13 (ddd, $^{3}J_{H–H}$= 7.4 Hz, $^{3}J_{H–H}$= 4.9 Hz, $^{4}J_{H–H}$= 1.2 Hz, 1H), 3.94 (s, 4H), 3.90 (s, 2H). ^{13}C NMR ($CDCl_3$, 100 MHz): δ 160.13, 159.17, 149.25, 142.69, 136.68, 136.50, 132.10, 128.95, 128.38, 125.77, 123.06, 122.36, 122.15, 122.03, 89.14, 88.81, 60.30, 60.22. HRMS (ESI/[M+H]$^+$) calcd. for $C_{34}H_{26}N_4$: 491.2230. Found: 491.2227.

Table 2 Information of type *i–xii*.

type	#	H···A (Å)	D···A (Å)	∠D–H···A (°)
i	16	2.32–2.70	3.32–3.76	135.6–163.2
ii	1	2.74	3.45	123.3
iii	8	2.54–2.78	3.48–3.65	129.4–144.5
iv	2	2.34, 2.75	3.38, 3.49	159.6, 125.1
v	24	2.56–2.90	3.22–3.91	99.7–157.1
vi	2	2.78, 2.81	3.50, 3.51	123.1, 122.0
vii	5	2.79–2.90	3.41–3.74	114.8–146.5
viii	1	(3.25)[a]	–	–
ix	1	2.67	3.54	137.1
x	3	2.62–2.75	3.57–3.68	142.4–151.0
xi	6	2.67–2.89	3.52–3.76	129.2–139.7
xii	1	2.51	3.41	140.2
Total 70		avg. 2.71	avg. 3.59	avg. 139.2

[a] The distance between two phenyl rings.

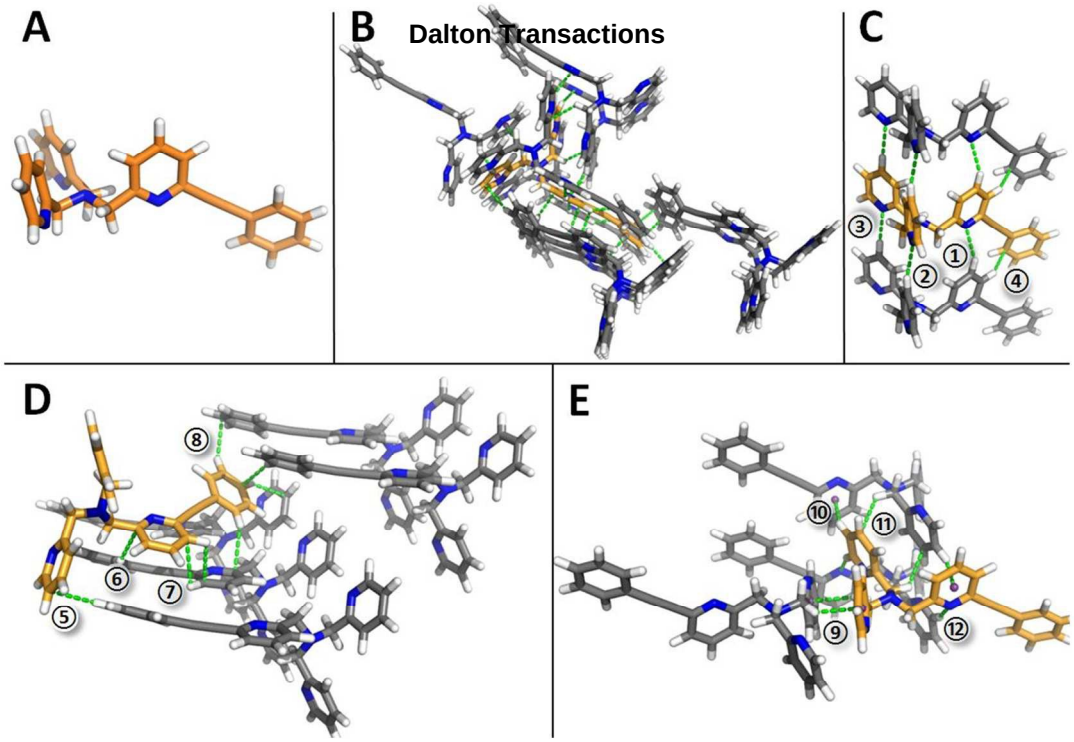

Fig. 2 (A) Crystal structure of the monomer of compound **1**. (B) Intermolecular short contacts of a molecule **1** with five other molecules and the details (C), (D), (E) *Contact 1*: type *i*, N···H–C 2.51 Å, N···C 3.48 Å, ∠N···H–C 148.3°. *Contact 2*: type *i*, N···H–C 2.36 Å, N···C 3.41 Å, ∠N···H–C 162.1°. *Contact 3*: type *i*, N···H–C 2.42 Å, N···C 3.45 Å, ∠N···H–C 156.8°. *Contact 4*: type *v*, C···H–C 2.75 Å, C···C 3.70 Å, ∠C···H–C 145.4°. *Contact 5*: type *v*, C···H–C 2.84 Å, C···C 3.77 Å, ∠C···H–C 144.2°. *Contact 6*: type *v*, C···H–C 2.81 Å, C···C 3.71 Å, ∠C···H–C 139.2°. *Contact 7*: type *v*, C···H–C 2.86 Å, C···C 3.22 Å, ∠C···H–C 99.7°. *Contact 8*: type *v*, C···H–C 2.85 Å, C···C 3.82 Å, ∠C···H–C 149.2°. *Contact 9*: type *ix*, $Py_{centroid}$···H–C 2.67 Å, $Py_{centroid}$···C 3.54 Å, ∠$Py_{centroid}$···H–C 137.1°. *Contact 10*: type *iii*, C–H···$Py_{centroid}$ 2.54 Å, C···$Py_{centroid}$ 3.48 Å, ∠C–H···$Py_{centroid}$ 144.1°. *Contact 11*: type *xi*, C···H–C 2.89 Å, C···C 3.67 Å, ∠C···H–C 129.2°. *Contact 12*: type *i*, N···H–C 2.70 Å, N···C 3.76 Å, ∠N···H–C 163.2°. C—orange and gray, H—white, N—blue and centroid—violet purple.

Compound 3. A 50 mL round-bottom flask was charged with DIPEA (372 mg, 2.88 mmol), compound **9** (392 mg, 1.44 mmol), and 20 mL of THF. The solution of compound **11** (150 mg, 0.720 mmol) in 5 mL of THF was added dropwise to the flask, and the mixture was stirred for 3 days at room temperature (20 °C). The white solid product was afforded in 53% yield (224 mg, 0.379 mmol) with the general method. The compound **3** started decomposing at 166 °C, and completely melted at 198 °C. ^{1}H NMR ($CDCl_3$, 400 MHz): δ 7.67 (dd, $^3J_{H–H}$= 7.8 Hz, $^3J_{H–H}$= 7.6 Hz, 3H), 7.63–7.56 (m, 9H), 7.41 (dd, $^3J_{H–H}$= 7.6 Hz, $^4J_{H–H}$= 1.1 Hz, 3H), 7.35 (m, 3H), 3.96 (s, 6H). ^{13}C NMR ($CDCl_3$, 100 MHz): δ 159.98, 142.76, 136.70, 132.13, 128.97, 128.40, 125.83, 122.36, 122.09, 89.21, 88.81, 60.25. HRMS (ESI/[M+Na]$^+$) calcd. for $C_{42}H_{30}N_4$: 613.2360. Found: 613.2370.

General method for compounds 4–6.[44] **Compound 4 [Cu(1)(MeOH)]·2ClO$_4$**. A 10 mL vial was charged with a solution of compound **1** (30 mg, 0.077 mmol) in 1.5 mL of anhydrous MeOH. A solution of Cu(II) perchlorate (29 mg, 0.077 mmol) in 1.0 mL of anhydrous MeOH was added dropwise to the prepared solution, and the mixture was stirred for 10 minutes at room temperature (20 °C). A blue sticky precipitate was formed upon addition of Et_2O (8.0 mL). A stirrer was kept on for additional 1 hour, and then left off for 30 minutes. The blue product clung to the wall of the vial. The solvent was poured out, and the residue was concentrated in vacuo to dryness. The gummy product was dissolved in 1 mL of MeOH. Single crystals of compound **4** were grown by slowly diffusing Et_2O into the solution in MeOH and collected with 85% yield (32 mg, 0.066 mmol). The compound **4** started decomposing at 78 °C, and completely melted at 145 °C.HRMS (ESI/[M]$^+$) calcd. for $C_{26}H_{22}N_4Cu$: 453.1135. Found: 453.1133.

Compound 5 [Cu(2)(MeCN)]·2ClO$_4$. A 10 mL vial was charged with the solution of compound **2** (30 mg, 0.061 mmol) in 1.5 mL of anhydrous MeOH. A solution of Cu(II) perchlorate (23 mg, 0.061 mmol) in 1.0 mL of anhydrous MeOH was added dropwise to the prepared solution, and the mixture was stirred for 10 minutes at room temperature (20 °C). A greenish blue precipitate was formed upon addition of Et_2O (8.0 mL), and collected by filtration. Single crystals of compound **5** were grown by slowly diffusing Et_2O into a solution in MeCN (1.0 mL) and collected with 95% yield (28 mg, 0.047 mmol). The compound **5** started decomposing at 176 °C, and melted in the range of 219–227 °C. HRMS (ESI/[M]$^+$) calcd. for $C_{34}H_{26}N_4Cu$: 553.1448. Found: 553.1420.

Compound 6 [Cu(3)(MeCN)]·2ClO$_4$. A 10 mL vial was charged with a solution of compound **3** (30 mg, 0.051 mmol) in 1.5 mL of anhydrous MeOH. A solution of copper(II) perchlorate (19 mg, 0.051 mmol) in 1.0 mL of anhydrous MeOH was added dropwise to the prepared solution, and the mixture was stirred for 10 minutes at room temperature (20 °C). A green precipitate was formed upon addition of Et_2O (8.0 mL), and collected by filtration. Single crystals of compound **6** were afforded by slowly diffusing Et_2O into s solution in MeCN (1.0 mL) and collected in 85% yield (30 mg, 0.045 mmol). The compound **6** started decomposing at 125 °C, and melted in the range of 193–199 °C. HRMS (ESI/[M]$^+$) calcd. for $C_{42}H_{30}N_4Cu$: 653.1761. Found: 653.1766.

Crystallization conditions. Single crystals of compounds **1**–**3** were formed by slowly diffusing a CH_2Cl_2 solution into

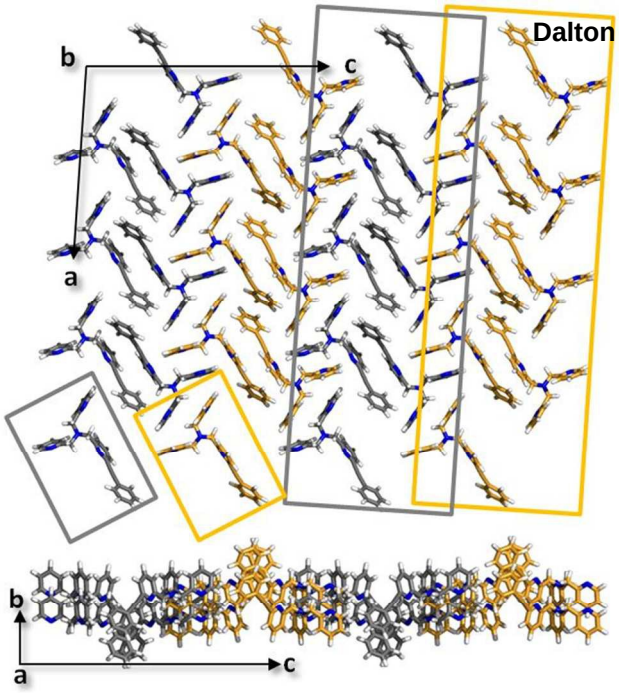

Fig. 3 2D layer ($a\times b\times c$ = 2×1×2) viewed from *b* axis and its side-view from *a* axis for compound **1**. Molecules in the same color face the same direction. The small rectangle is the top view of the columnar assembly, and the large one is the top view of the wall-like structure. C—orange and gray, H—white, and N—blue.

hexane. Each compound (50 mg) was dissolved into 2 mL of CH_2Cl_2, and carefully placed under 8 mL of hexanes in a 10 mL vial without disturbance to prevent a quick growth of crystal. The closed vial was put on a shelf. Single crystals of sufficiently high quality for X-ray diffraction were obtained in a couple of days.

Results and Discussion

Crystal structures

Seventy non-covalent interactions in six X-ray single crystal structures of **1**–**6** have been identified, and classified into twelve types of hydrogen-involved non-covalent interactions shown in Fig. 1. Except the type *viii* interaction that is a typical slipped π···π stack, eleven types of interactions are weak hydrogen bonds with 2.2–3.2 Å of hydrogen (H)···acceptor (A) bond lengths and 3.2–4.0 Å of donor (D)···A distances.[45] Table 2 shows the number of each type of interaction, the range of H···A bond lengths and D···A distances, as well as bond angles. Type *i* is the interaction between a C_{sp^2}–H of prydinyl/phenyl group and N_{sp^2} of pyridine ring, and is the strongest dipole-dipole interaction in this study. Sixteen of type *i* are observed in the crystal structures of **1**–**3**. The range of H···N distances in type *i* is 2.32–2.70 Å and that of C···N distances is 3.32–3.76 Å. The type *ii* interaction between the methyl C_{sp^3}–H and pyridyl N_{sp^2} was observed in the crystal structure of **2**. Type *i* and *ii* interactions between free lone-pair electrons of nitrogen and C–H are possible for the free ligand **1**–**3** but not for the basic nitrogens of **4**–**6** which form Cu–N bonds in their metal complexes.

Types *iii*–*xii* are interactions between an electron-deficient hydrogen and the aromatic π-system of Ph/Py or the conjugated π-system of Ph–C≡C–Py ligand. Type *iii* is a typical edge-to-face interaction between an aryl C–H and the centroid of an aryl group. Eight such interactions were found in the crystal structures of **1**–**3** with 2.54–2.78 Å of [C_{sp^2}–H···$Ar_{centroid}$] contacts and 3.48–3.65 Å of [C_{sp^2}···$Ar_{centroid}$] distances, in the range of weak hydrogen bonding. Two of type *iv* interactions, the contacts between C_{sp^2}–H and C=C of aryl group, are observed in the solid-state of complex **6**. One is the second shortest contact in this study; the length of H···C=$C_{centroid}$ is 2.34 Å and the distance of C···C=$C_{centroid}$ is 3.38 Å. The other is 2.75Å of H···A and 3.49 Å of D···A. One third of total non-covalent interactions are type *v*, [C_{sp^2}–H···C_{sp^2}] contacts. Twenty-four of type *v* interactions are found in five crystal structures, except that of **4** having only three pairs of short contacts. The shortest H···C_{sp^2} of type *v* is 2.56 Å and the longest one is 2.90 Å. The range of C_{sp^2}···C_{sp^2} length is 3.22–3.91 Å.

A carbon–carbon triple bond also participates in non-covalent interactions as a hydrogen bond acceptor in type *vi* and *vii* interactions. Two of type *vi* were observed in the crystal structure of **3**, in which two phenyl hydrogens contact the middle of a triple bond with bond lengths of 2.78 Å and 2.81 Å. Type *vii* is the short contact of the aryl hydrogen with the sp-carbon in triple bond, and five type *vii* interactions of 2.79–2.90 Å bond lengths were found in compounds **2**, **3**, and **5**. Type *viii* is an aromatic-aromatic interaction between two phenyl rings in the solid-state of **4**, that is, the interactions between the partially positive hydrogen of one phenyl ring and the centroid of another phenyl ring and vice versa. The hydrogen bond donor for types *ix*–*xii* is a sp^3-C–H of a methylene group that is between two of electron-withdrawing groups—a pyridyl group and an electronegative amine nitrogen. The methylene hydrogen forms eleven interactions with the π-system of Ph/Py or Ph–C≡C–Py ligand. Considering a ratio of methylene hydrogens to aryl hydrogens of six molecules in this study, type *ix*–*xii* interactions are of significance and comparable to type *iii*–*vii* in terms of H···C_{sp^2} bond length and the number of interactions. Type *xii* was found as a unique CH–π interaction, in which a methylene hydrogen contacts with three carbons [–C_{sp^2}=C_{sp^2}–C_{sp}≡] in the solid-state of **6**.

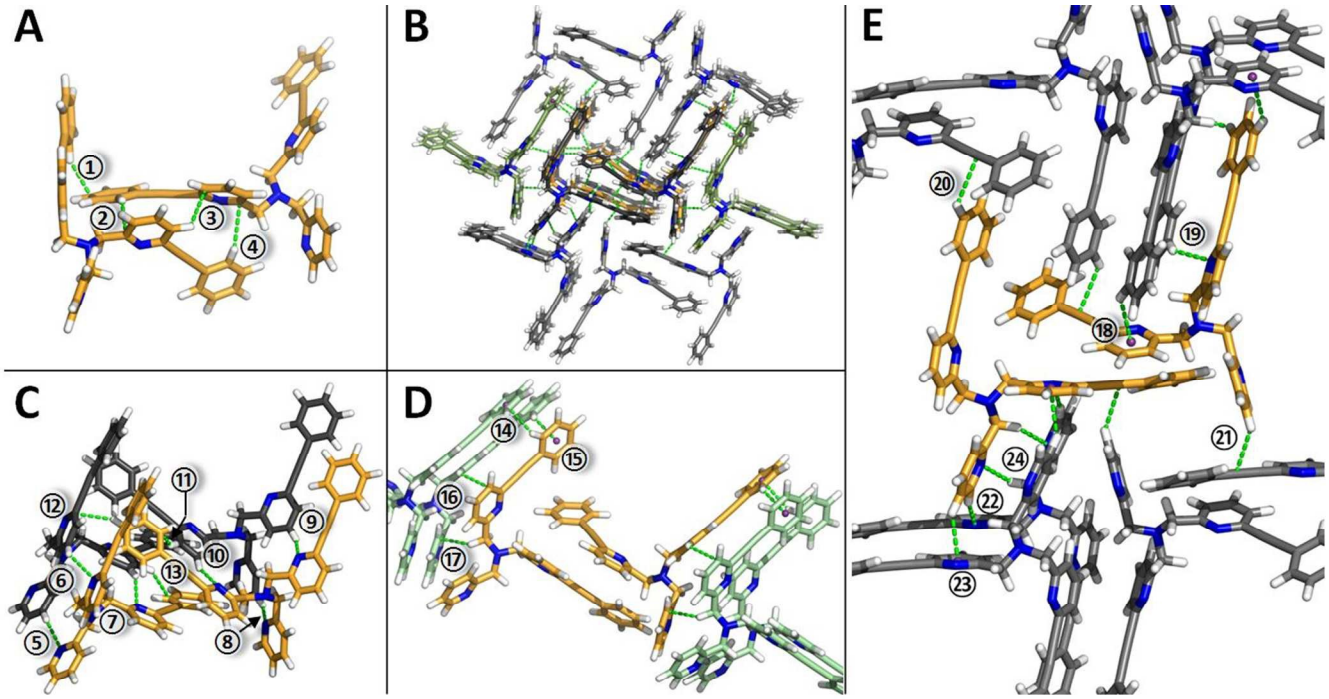

Fig. 4 (A) The asymmetric unit of compound **2** in its crystal structure and the short contacts in it. *Contact 1*: type *v*, C···H–C 2.56 Å, C···C 3.57 Å, ∠C···H–C 153.2°. *Contact 2*: type *v*, C···H–C 2.74 Å, C···C 3.62 Å, ∠C···H–C 137.9°. *Contact 3*: type *v*, C···H–C 2.80 Å, N···C 3.37 Å, ∠C···H–C 112.0°. *Contact 4*: type *v*, C···H–C 2.88 Å, C···C 3.81 Å, ∠C···H–C 142.7°. (B) Intermolecular short contacts of the asymmetric unit of molecule **2** with sixteen molecules and the details (C), (D), (E) *Contact 5*: type *i*, N···H–C 2.43 Å, N···C 3.42 Å, ∠N···H–C 150.6°. *Contact 6*: type *i*, N···H–C 2.66 Å, N···C 3.53 Å, ∠N···H–C 136.6°. *Contact 7*: type *i*, N···H–C 2.49 Å, N···C 3.45 Å, ∠N···H–C 145.6°. *Contact 8*: type *i*, N···H–C 2.45 Å, N···C 3.43 Å, ∠N···H–C 148.9°. *Contact 9*: type *i*, N···H–C 2.50 Å, N···C 3.45 Å, ∠N···H–C 145.5°. *Contact 10*: type *i*, N···H–C 2.37 Å, N···C 3.38 Å, ∠N···H–C 154.8°. *Contact 11*: type *v*, C···H–C 2.65 Å, C···C 3.59 Å, ∠C···H–C 144.6°. *Contact 12*: type *v*, C···H–C 2.70 Å, C···C 3.71 Å, ∠C···H–C 154.6°. *Contact 13*: type *v*, C···H–C 2.73 Å, C···C 3.65 Å, ∠C···H–C 141.9°. *Contact 14*: type *iii*, C–H···$Ph_{centroid}$ 2.74 Å, C···$Ph_{centroid}$ 3.53 Å, ∠C–H···$Ph_{centroid}$ 129.4°. *Contact 15*: type *iii*, C–H···$Ph_{centroid}$ 2.74 Å, C···$Ph_{centroid}$ 3.60 Å, ∠C–H···$Ph_{centroid}$ 135.5°. *Contact 16*: type *v*, C···H–C 2.89 Å, C···C 3.55 Å, ∠C···H–C 118.9°. *Contact 17*: type *xi*, C–H···C 2.89 Å, C···C 3.74 Å, ∠C–H···C 134.9°. *Contact 18*: type *iii*, $Py_{centroid}$···H–C 2.78 Å, $Py_{centroid}$···C 3.65 Å, ∠$Py_{centroid}$···H–C 136.9°. *Contact 19*: type *i*, N···H–C 2.68 Å, N···C 3.62 Å, ∠N···H–C 143.7°. *Contact 20*: type *vii*, C–H···C 2.90 Å, C···C 3.62 Å, ∠C–H···C 124.3°. *Contact 21*: type *vii*, C–H···C 2.84 Å, C···C 3.69 Å, ∠C–H···C 135.9°. *Contact 22*: type *i*, C–H···N 2.66 Å, C···N 3.70 Å, ∠C–H···N 161.1°. *Contact 23*: type *iii*, C–H···$Py_{centroid}$ 2.61 Å, C···$Py_{centroid}$ 3.55 Å, ∠C–H···$Py_{centroid}$ 144.5°. *Contact 24*: type *ii*, N···H–C 2.74 Å, N···C 3.45 Å, ∠N···H–C 123.3°. C—orange, pale green, dark gray and gray, H—white, N—blue and centroid—violet purple.

Although a tertiary amine nitrogen is the most basic in compounds **1**–**3**, it astonishingly does not participate in any supramolecular non-covalent interaction due to the steric hinderance of the pyridyl groups. The intermolecular short contact of the amine nitrogen with the hydrogen at 3-position of pyridyl group was not observed in the solid-state of **1**–**3**. However, those hydrogens are placed on top of the lone-pair electrons of the nitrogen atom, and prevent the nitrogen from the approach of the partial positive species.

Compound 1. X-ray determined crystal structures of compound **1** show it arranges in a monoclinic crystal system with a *C* 2/c space group (Fig. 2). The asymmetric unit of the crystal structure contains one molecule of **1**, and its unit cell consists of eight molecules of **1** with no solvent molecule. In the solid state, the lone-pair electrons of the nitrogen of the central amine align opposite to those of the pyridyl nitrogens to minimize repulsive interactions among electron-rich nitrogens (Fig. 2A). Dihedral angles between the plane containing three methylene carbons and each pyridine ring are in the range of 76.0–81.6°. The carbon–carbon triple bond is nearly linear, with C–C≡C angles of 176.1° and 177.2°. Possessing the conformational properties mentioned above, each molecule of **1** closely contacts ten of its neighbours, through twelve pairs of hydrogen bonding interactions classified into type *i*, *iii*, *v*, *ix*, and *xi* (Fig. 2B). Three pyridine moieties of the molecule establish short [N_{sp^2}···H–C_{sp^2}] contacts (contact 1–3 in Fig. 2C, 2.51, 2.36, and 2.42 Å, type *i*) with their counterparts of top and bottom molecules. The *ortho* carbon of terminal phenyl group engages into a weak [C_{sp^2}–H···C_{sp^2}] hydrogen bond (contact 4 in Fig. 2C, 2.75 Å, type *v*) with the hydrogen atom on the adjacent pyridine ring. Eight pairs of contacts, 5–12, can be identified between the other eight peripheral molecules and the central orange-coloured molecule (Fig. 2D & 2E): (1)–(4) the short [C_{sp^2}···H–C_{sp^2}] contacts between aromatic carbons and aromatic hydrogens (contact 5–8, 2.84 Å, 2.81 Å, 2.86 Å, and 2.85 Å, type *v*); (5) the pairwise [C_{sp^3}–H···$Py_{centroid}$] contacts between the methylene hydrogen and the π electrons of pyridyl ring (contact 9, 2.67 Å, type *ix*); (6) the CH–π interaction [C_{sp^2}–H···$Py_{centroid}$] between the pyridyl hydrogen and the π electrons of pyridine ring (contact 10, 2.54 Å, type *iii*); (7) the short

$[C_{sp^3}–H\cdots C_{sp^2}]$ contact between methylenyl hydrogen and

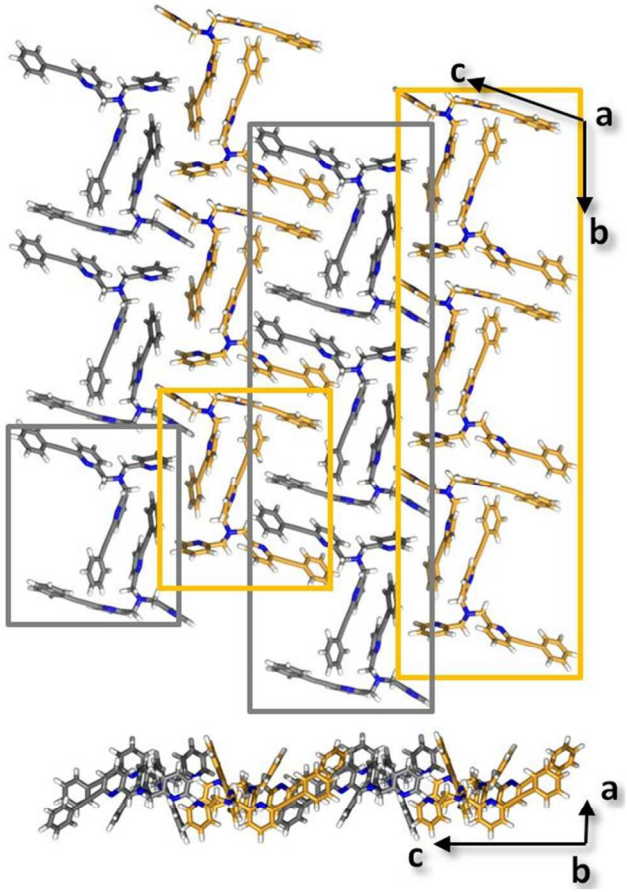

Fig. 5 2D layer ($a\times b\times c$ = 1×3×2) viewed from *a* axis and its side-view from *b* axis for compound **2**. Molecules in the same color face the same direction. The small rectangle is the top view of the columnar assembly, and the large one is the top view of the wall-like structure. C—orange and gray, H—white, and N—blue.

aromatic carbon of pyridine group (contact 11, 2.89 Å, type *xi*); (8) the pairwise $[N_{sp^2}\cdots H–C_{sp^2}]$ contacts between the pyridyl nitrogen and the *ortho* pyridyl hydrogen (contact 12, 2.70 Å, type *i*). Compound **1** assembles into a columnar structure through contacts 1–4, where the column is a part of a wall-like structure formed through contacts 5–8 among columns facing the same direction. Fig. 3 shows the top view of four wall-structures in two colours: the small rectangles are the top view of two columns that they face opposite direction; the large rectangles are the top view of two walls that consist of columns in the same colours. The two walls in different colour are combined with contacts 9–12.

Compound 2. Compound **2** crystallizes in $P\bar{1}$ triclinic space group, with four molecules of **2** in the unit cell, and two molecules in the asymmetric unit, in which two molecules face the same direction (Fig. 4A). The solid-state structure of compound **2** shows a similar conformation with compound **1**. Dihedral angles between the plane containing three methylene carbons and each pyridine ring for each monomer in the asymmetric unit are in the range of 63.9–85.2° and the bond angles of C–C≡C are between 173.1° and 179.3°. Two molecules in the asymmetric unit are combined with each other through contacts 1–4, with four contacts as CH···π interactions

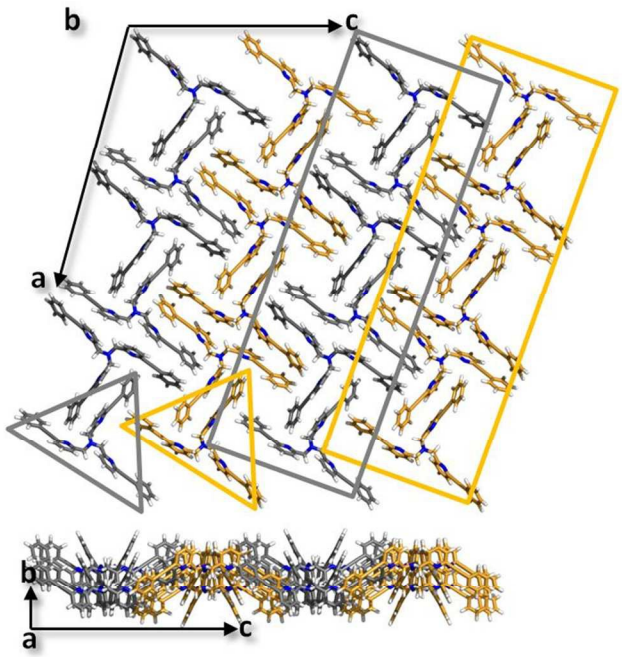

Fig. 6 2D layer ($a\times b\times c$ = 2×1×2) viewed from *b* axis and its side-view from *a* axis for compound **3**. Molecules in the same color face the same direction. The triangles are the top view of the columnar assemblies, and the rectangles are the top view of the wall-like structures. C—orange and gray, H—white, and N—blue.

in the moderate length of 2.56, 2.74, 2.80, and 2.88 Å of $[C_{sp^2}–H\cdots C_{sp^2}]$, respectively (Fig. 4A). The asymmetric unit (orange-coloured carbon) has twenty pairs of short contacts with sixteen molecules where contacts are classified into type *i*, *ii*, *iii*, *v*, *vii*, and *xi* (Fig. 4B). The cluster of molecules gathered around orange-coloured asymmetric unit divides into three parts—two asymmetric units in dark gray (Fig. 4C, the asymmetric unit on upper layer was omitted.), four molecules in pale green to the east and the west (Fig. 4D), and eight molecules in gray to the north and the south (Fig. 4E). Molecules in dark gray and the central orange unit are connected to each other through nine interactions; six $[N_{sp^2}\cdots H–C_{sp^2}]$ contacts of hydrogen bonding type *i* (contact 5–10 in Fig. 4C, 2.43, 2.66, 2.49, 2.45, 2.50, and 2.37 Å) and three $[C_{sp^2}\cdots H–C_{sp^2}]$ contacts of type *v* (contact 11–13 in Fig. 4C, 2.65, 2.70, and 2.73 Å). The interactions between four pale green molecules and the orange unit are four pairs of CH···π interactions; two $[C_{sp^2}–H\cdots Ph_{centroid}]$ contacts (contact 14 & 15, 2.74 Å, type *iii*), a $[C_{sp^2}–H\cdots C_{sp^2}]$ contact (contact 16, 2.89 Å, type *v*), and a $[C_{sp^3}–H\cdots C_{sp^2}]$ contact (contact 17, 2.89 Å, type *xi*) (Fig. 4D). Seven pairwise interactions in four types link eight gray-coloured molecules to the central asymmetric unit; two $[N_{sp^2}\cdots H–C_{sp^2}]$ contacts (contact 19 & 22, 2.68 Å & 2.66 Å, type *i*), a $[N_{sp^2}\cdots H–C_{sp^3}]$ contact (contact 24, 2.74 Å, type *ii*), two $[C_{sp^2}–H\cdots Py_{centroid}]$ contacts (contact 18 & 23, 2.78 Å & 2.61 Å, type *iii*), and two $[C_{sp^2}–H\cdots C_{sp}]$ contacts (contact 20 & 21, 2.90 Å & 2.84 Å, type *vii*) (Fig. 4E). The asymmetric unit assembles into a column-like structure via contacts 5–10, and the columnar structures are lined up in a row through contacts 14–17 to complete a wall-like structure shown in Fig.

5. Each orange-coloured wall establishes short contacts 18–24 with gray-coloured walls in Fig. 5.

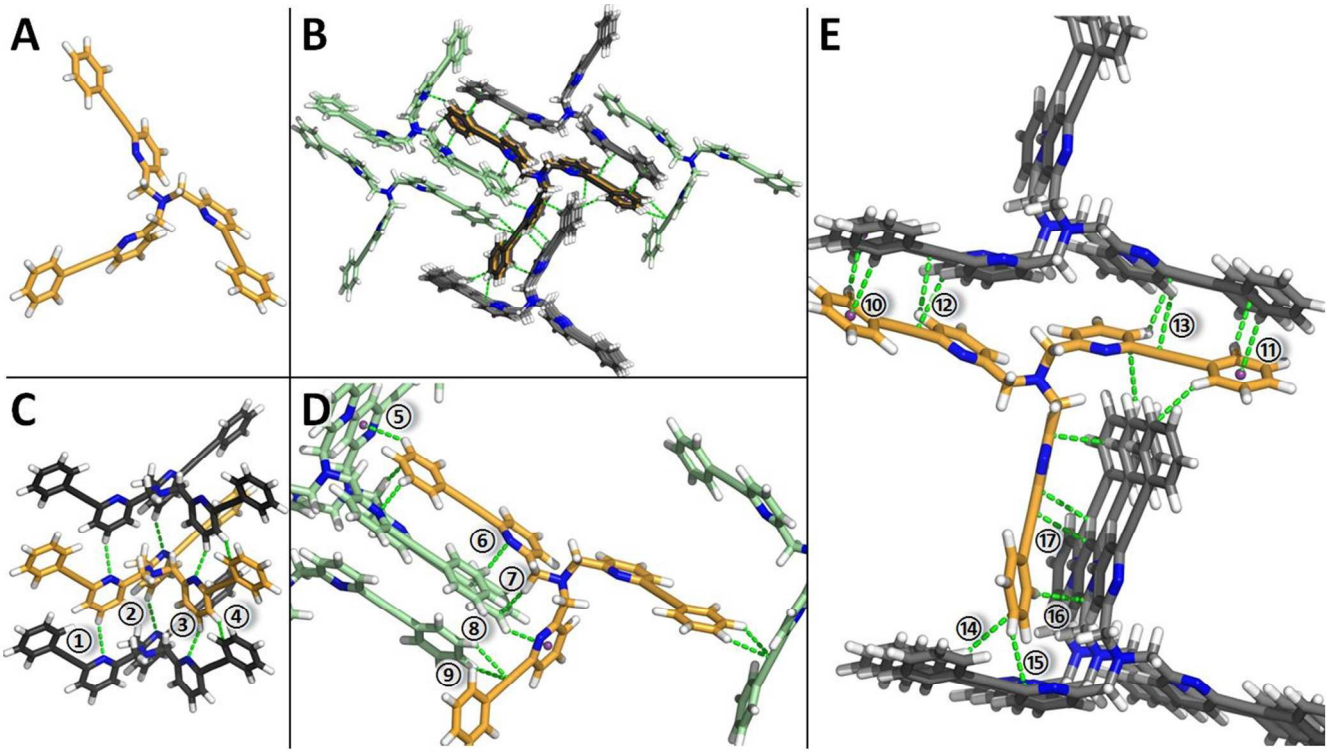

Fig. 7 (A) Crystal structure of the monomer of compound **3**. (B) Intermolecular short contacts of a molecule **3** with ten molecules and the details (C), (D), and (E). *Contact 1*: type *i*, C–H···N 2.60 Å, C···N 3.47 Å, ∠C–H···N 135.9°. *Contact 2*: type *i*, C–H···N 2.61 Å, C···N 3.47 Å, ∠C–H···N 135.6°. *Contact 3*: type *i*, C–H···N 2.32 Å, C···N 3.32 Å, ∠C–H···N 151.5°. *Contact 4*: type *v*, C–H···C 2.69 Å, C···C 3.63 Å, ∠C–H···C 144.4°. *Contact 5*: type *iii*, C–H···$Py_{centroid}$ 2.70 Å, C···$Py_{centroid}$ 3.62 Å, ∠C–H···$Py_{centroid}$ 141.9°. *Contact 6*: type *i*, N···H–C 2.57 Å, N···C 3.54 Å, ∠N···H–C 147.6°. *Contact 7*: type *xi*, C–H···C 2.86 Å, C···C 3.76 Å, ∠C–H···C 139.7°. *Contact 8*: type *vi*, C–H···C≡$C_{centroid}$ 2.81 Å, C···C 3.51 Å, ∠C–H···C 122.0°. *Contact 9*: type *vi*, C–H···C≡$C_{centroid}$ 2.78 Å, C···C 3.50 Å, ∠C–H···C 123.1°. *Contact 10*: type *iii*, C–H···$Ph_{centroid}$ 2.68 Å, C···$Ph_{centroid}$ 3.49 Å, ∠C–H···$Ph_{centroid}$ 131.6°. *Contact 11*: type *iii*, C–H···$Ph_{centroid}$ 2.71 Å, C···$Ph_{centroid}$ 3.54 Å, ∠C–H···$Ph_{centroid}$ 132.2°. *Contact 12*: type *vi*, C···H–C 2.86 Å, C···C 3.59 Å, ∠C···H–C 124.0°. *Contact 13*: type *vii*, C···H–C 2.81 Å, C···C 3.41 Å, ∠C···H–C 114.8°. *Contact 14*: type *v*, C–H···C 2.84 Å, C···C 3.79 Å, ∠C–H···C 145.6°. *Contact 15*: type *v*, C–H···C 2.88 Å, C···C 3.91 Å, ∠C–H···C 157.1°. *Contact 16*: type *v*, C–H···C 2.78 Å, C···C 3.66 Å, ∠C–H···C 138.1°. *Contact 17*: type v, C–H···C 2.87 Å, C···C 3.86 Å, ∠C–H···C 106.6°. C—orange, pale green, dark gray and gray, H—white, N—blue and centroid—violet purple.

Compound 3. Compound **3** crystallizes in a monoclinic crystal system with a *C* 2/c space group (Fig. 7). The asymmetric unit of the crystal structure contains one molecule of **3**, and its unit cell has eight molecules of **3** and four disordered molecules of CH_2Cl_2 (subtracted using the PLATON/SQUEEZE routine). Dihedral angles between the plane containing three methylene carbons and each pyridine ring are in the range of 68.0–83.6°. Carbon–carbon triple bonds of **3** are virtually undeformed, with C–C≡C angles of 176.1° and 177.2°. The central orange molecule in Fig. 7B contacts eleven of its neighbours, through seventeen pairs of short contacts classified into type *i*, *iii*, *v*, *vi*, *vii*, and *xi*. The supramolecular structure of **3** is highly reminiscent of that of **1** and **2**, as the compound assembles into one-dimensional structures lined up in a row to build two-dimensional assembly that completes three-dimensional crystal (Fig. 6). The columnar structure is build up via four pairs of short contacts between the orange-coloured molecule and the dark-gray-coloured molecules in Fig. 7C; three [C_{sp^2}–H···N_{sp^2}] contacts (contacts 1–3, 2.60, 2.61, and 2.32 Å, type *i*) and a [C_{sp^2}–H···C_{sp^2}] contact (contact 4, 2.69 Å, type *v*). Four molecules in pale green are connected to the orange molecule by five couples of short contacts in four types of interactions in Fig. 7D; type *i* (contact 6, [N_{sp^2}···H–C_{sp^2}], 2.57 Å), type *iii* (contact 5, [C_{sp^2}–H···$Py_{centroid}$], 2.70 Å), type *vi* (contact 8 & 9, [C_{sp^2}–H···C≡$C_{centroid}$], 2.81 & 2.87 Å), and type *xi* (contact 7, [C_{sp^3}–H···C_{sp^2}], 2.86 Å). The interactions shown in Fig. 7D combine the wall-like structures in Fig. 6 with a combination of columnar structures with contacts 10–17 in Fig. 7E. These eight contacts are classified into three types—two [$Ph_{centroid}$···H–C_{sp^2}] contacts in type *iii* (contacts 10 & 11, 2.68 & 2.71 Å), four [$_{Csp^2}$–H···C_{sp^2}] contacts in type *v* (contacts 14–17, 2.84, 2.88, 2.78, and 2.87 Å), and two [C_{sp}···H–C_{sp^2}] contacts in type *vii* (contacts 12 & 13, 2.86 & 2.81 Å).

Compound 4. Compound **4**, [Cu(**1**)MeOH]·$2ClO_4$, crystallizes in a monoclinic crystal system with a *P* 2_1/n space group (Fig. 8), and its unit cell has four asymmetric units which contain a [Cu(**1**)MeOH]·$2ClO_4$ complex, shown in Fig. 8A. The copper(II) cation ties four basic nitrogens of the molecule **1** as a tetradentate ligand, and fills its empty binding site with a methanol molecule as solvent. As all ligands are electronically neutral, two perchlorate anions bind to the cationic $Cu(\mathbf{1})^{2+}$ complex through ion-dipole interactions. The Cu–O bond length, 1.97 Å, is shorter than four Cu–N bonds in the complex:

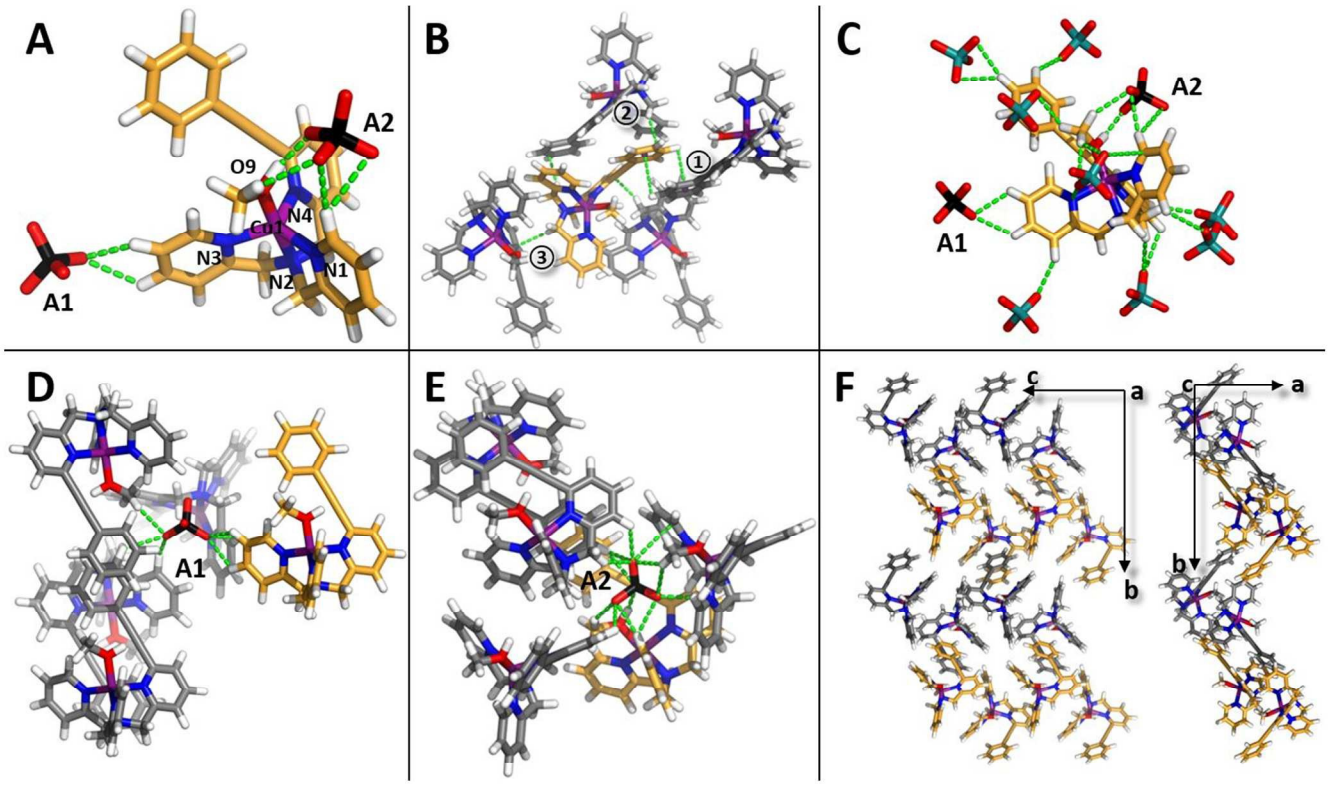

Fig. 8 (A) Crystal structure of the asymmetric unit of compound **4** [Cu(**1**) MeOH]·2ClO_4. (B) Intermolecular short contacts of the cationic Cu^{2+} complex **4** with four other Cu^{2+} complexes. *Contact 1*: type *viii*, π···π 3.25 Å. *Contact 2*: type *x*, C–H···C=$C_{centroid}$ 2.64 Å, C···C=$C_{centroid}$ 3.57 Å, ∠C–H···C=$C_{centroid}$ 142.4°. *Contact 3*: type *xi*, C–H···C 2.67 Å, C···N 3.56 Å, ∠C–H···C 139.3°. (C) Nineteen short contacts of cationic Cu^{2+} complex with ten of perchlorate anions. (D) Six short contacts of anion A1 with five of cationic Cu^{2+} complexes, and (E) Thirteen short contacts of anion A2 with five of cationic Cu^{2+} complexes. (F) 2D layer (*a*×*b*×*c* = 1×2×2) viewed from *a* axis that molecules in orange face forward and those in gray face backward, and its side-view from *c* axis for complex 4. Anions are omitted for clarity. C—orange and gray, H—white, N—blue, O—red, Cl—black and deep teal, Cu—deep purple, and centroid—violet purple.

2.02 Å of Cu–N1, 2.00 Å of Cu–N2, 2.03 Å of Cu–N3, and 2.17 Å of Cu–N4. Dihedral angles between the plane containing three methylene carbons and each pyridine ring are in the range of 68.7–83.8°. C_{Ph}–C≡C–C_{Py} is almost linear with C–C≡C angles of 178.2° and 178.3°. Although ten of perchlorate anions surround a cationic complex (Fig. 8C), three pairs of short contacts between the central orange [Cu(**1**)MeOH]$^{2+}$ complex and its four neighbouring complexes are observed (Fig. 8B). Contact 1 is a typical slipped π···π stack with a distance of 3.25 Å. Two types of C–H···π interactions also connect cationic species together; a [C_{sp^3}–H···C=$C_{centroid}$] interaction (contact 2, 2.64 Å, type *x*) and a [C_{sp^3}–H···C] interaction (contact 3, 2.67 Å, type *xi*). As each cationic Cu(**1**)$^{2+}$ complex is surrounded by ten perchlorate anions, each perchlorate is surrounded by five cationic complexes (Fig. 8D and 8E). While anion A1 conjoins five [Cu(**1**)MeOH]$^{2+}$ complexes via six ion-dipole interactions [C–H···O] with the distances between 2.35 Å and 2.72 Å, the anion A2 holds them with thirteen short contacts. The shortest contact between A2 and cationic complex is the [O–H···O] interaction of 1.83 Å, and the longest one is the [C_{sp^2}···O] interaction of 3.20 Å. The second longest one is 3.00 Å between the pyridyl nitrogen and the oxygen of anion. The rest of the ten contacts are ion-dipole [C–H···O] interactions with the distances between 2.43 Å and 2.71 Å. A total of twenty-two non-covalent interactions comprised of π···π stacking, dipole-dipole, and ion-dipole interactions are found in the crystal of complex **4**, [Cu(**1**)MeOH]·2ClO_4(Fig. 8F).

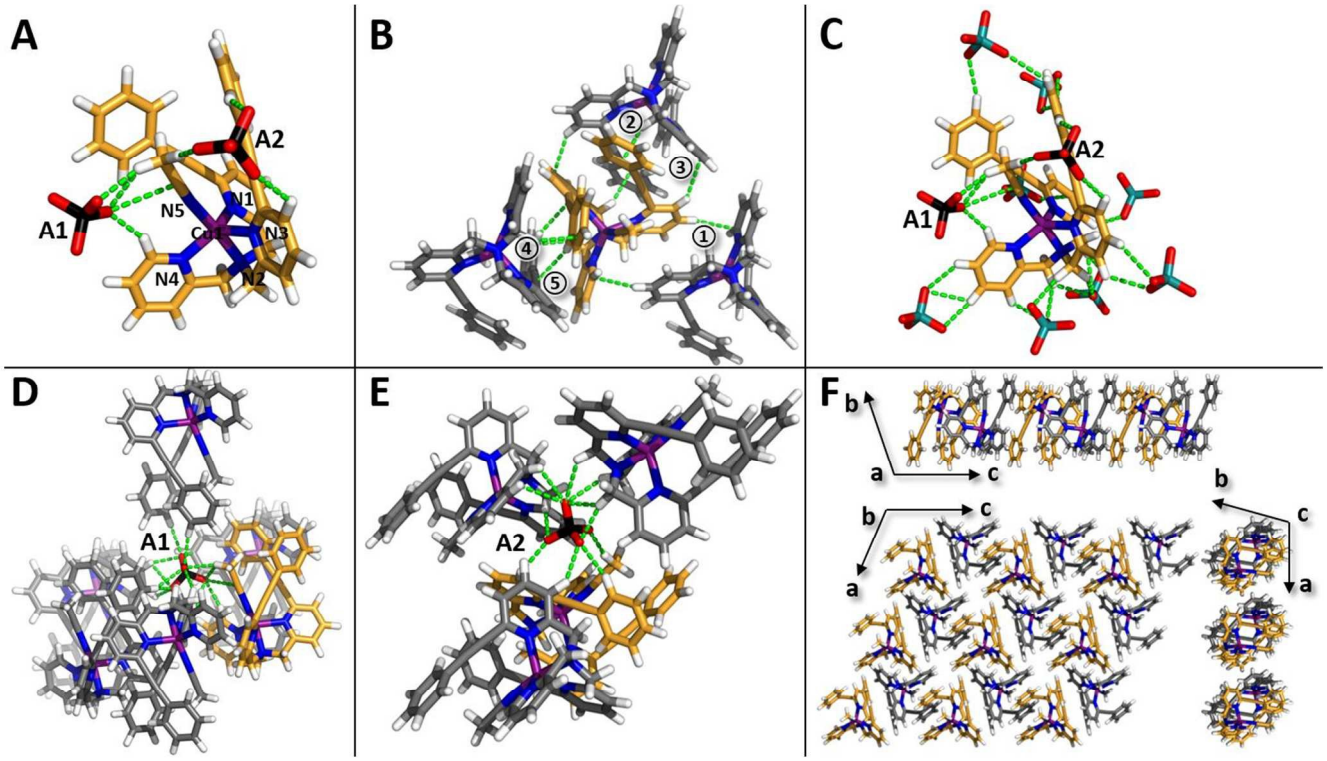

Fig. 9 (A) Crystal structure of the asymmetric unit of compound **5** [Cu(**2**) MeCN]·2ClO_4. (B) Intermolecular short contacts of the cationic Cu^{2+} complex **5** with three other Cu^{2+} complexes. *Contact 1*: type *v*, C–H···C 2.84 Å, C···C 3.72 Å, ∠C–H···C 137.6°. *Contact 2*: type *x*, C–H···C=$C_{centroid}$ 2.62 Å, C···C=$C_{centroid}$ 3.61 Å, ∠C–H···C=$C_{centroid}$ 151.0°. *Contact 3*: type *v*, C–H···C 2.84 Å, C···C 3.77 Å, ∠C–H···C 143.7°. *Contact 4*: type *x*, C–H···C=$C_{centroid}$ 2.75 Å, C···C=$C_{centroid}$ 3.68 Å, ∠C–H···C=$C_{centroid}$ 143.4°. *Contact 5*: type *vii*, C–H···C 2.79 Å, C···C 3.74 Å, ∠C–H···C 146.5°. (C) Twenty-five short contacts of cationic Cu^{2+} complex with ten of perchlorate anions. (D) Fourteen short contacts of anion A1 with six of cationic Cu^{2+} complexes, and (E) Eleven short contacts of anion A2 with four of cationic Cu^{2+} complexes. (F) 2D layer ($a \times b \times c = 3 \times 1 \times 3$) viewed from *b* axis that molecules in orange face forward and those in gray face backward, and its top-view from *a* axis and its side-view from *c* axis for complex **4**. Anions are omitted for clarity. C—orange and gray, H—white, N—blue, O—red, Cl—black and deep teal, and Cu—deep purple.

Compound 5. Compound **5**, [Cu(**2**)MeCN]·2ClO_4, crystalizes in a triclinic system with a $P\bar{1}$ space group (Fig. 9). Its unit cell has two asymmetric units which contain a [Cu(**2**)MeCN]·2ClO_4 complex, shown in Fig. 9A. The molecule **2,** as a tetradentate ligand, binds to copper(II) with its tertiary amine and three pyridine moieties, and an acetonitrile molecule fills the empty binding site. As all ligands are electronically neutral, two perchlorate anions bind to the cationic Cu(**2**)$^{2+}$ complex through ion-dipole interactions. The bond length of Cu–N5, 1.96 Å, is the shortest Cu–N bond in the complex **5**: 2.14 Å of Cu–N1, 2.00 Å of Cu–N2, 2.10 Å of Cu–N3, and 2.03 Å of Cu–N4. Dihedral angles between the plane containing three methylene carbons and each pyridine ring are in the range of 60.9–78.5°. Two of C_{Ph}–C≡C–C_{Py} are slightly deformed with C–C≡C angles of 175.1°, 178.7°, 176.9°, and 177.2°. The [Cu(2)MeCN]$^{2+}$ complex in orange colour in Fig. 9B is surrounded by three neighbours of cationic complexes via five pairs of short contacts: two [C_{sp^2}–H···C_{sp^2}] contacts (contact 1 & 3, 2.84 Å for both, type *v*), two [C_{sp^3}–H··C=$C_{centroid}$] contacts (contact 2 & 4, 2.62 Å & 2.75 Å, type *x*), and a [C_{sp^2}–H···C_{sp}] contact (contact 5, 2.79 Å, type *vii*). A [Cu(**2**)MeCN]$^{2+}$ cation associates with ten perchlorate anions through twenty-five short contacts (Fig. 9C) divided into two groups—fourteen short contacts of anion A1 with six of cationic Cu^{2+} complexes (Fig. 9D), and eleven short contacts of anion A2 with four of cationic Cu^{2+} complexes (Fig. 9E). Except for two [C···O] contacts (3.17 Å & 3.20 Å) between A1 and ligand 2, the average distance of twelve [C–H···O] contacts of A1 is 2.50 Å, which is slightly longer than that (2.46 Å) of eleven [C–H···O] contacts of A2. The 3D assembly of complex **5** (Fig. 9F) is governed by thirty non-covalent interactions; primarily ion-dipole interactions and dipole-dipole interactions.

Compound 6. Compound **6**, [Cu(**3**)MeCN]·2ClO_4, also assembled into a triclinic crystal system with a $P\bar{1}$ space group (Fig. 10). Its unit cell has two asymmetric units which contain a [Cu(**3**)MeCN]·2ClO_4 complex, shown in Fig. 10A. The molecule **3**, as a tetradentate ligand, binds to copper(II) cation with one tertiary amine and three pyridine moieties, with an acetonitrile filling the empty binding site of copper(II) cation. As all ligands are electronically neutral, two perchlorate anions bind to the cationic Cu(**3**)$^{2+}$ complex through ion-dipole interactions. The bond length of Cu–N5, 1.94 Å, is the shortest Cu–N bond in the complex **6**: 2.18 Å of Cu–N1, 1.98 Å of Cu–N2, 2.10 Å of Cu–N3, and 2.05 Å of Cu–N4. Dihedral angles between the plane containing three methylene carbons and each pyridine ring are in the range of 63.5–73.1°. One of C_{Ph}–C≡C–C_{Py} is remarkably deformed with C–C≡C angle of 168.7° and 174.7°. Two other ethynyl groups are also slightly deformed with C–C≡C angles from 174.0° to 177.7°. The [Cu(**3**)MeCN]$^{2+}$ complex (orange) is surrounded by six neighbours of cationic

complexes via nine pairs of short contacts classified into four types of interactions (Fig. 10B). Fig. 10D shows six pairs of short contacts (orange complex) with three gray-coloured neighbours; two [C_{sp^3}–H···C_{sp^2}] contacts (contact 1 & 5, 2.84 Å & 2.72 Å, type *xi*), two [C_{sp^2}–H···C=$C_{centroid}$] contacts (contact 2 & 3, 2.75 Å & 2.34 Å, type *iv*), a [C_{sp^3}–H···C=C–$C_{centroid}$] contact (contact 4, 2.51 Å, type *xii*), and a [C_{sp^2}–H···C_{sp^2}] contact (contact 6, 2.65 Å, type *v*). The Cu^{2+} complex also has additional three pairs of contacts in type *v* with two complexes (pale-green), and one complex (dark-gray) (contact 7–9, 2.90 Å, 2.78 Å, and 2.84 Å, in Fig. 10E). As shown in X-ray crystal structure of complex **5**, a [Cu(**3**)MeCN]$^{2+}$ cation also associates with ten perchlorate anions through eighteen short contacts (Fig. 10C) divided into two groups—eleven short contacts of anion A1 with six cationic Cu^{2+} complexes (Fig. 10F), and seven short contacts of anion A2 with four cationic Cu^{2+} complexes (Fig. 10G). Eleven contacts between A1 and ligand **3** are [C–H···O] ion-dipole interactions in the range of distances 2.37–2.63 Å (average 2.52 Å). For A2, seven of [C–H···O] ion-dipole interactions are observed in the range of distances 2.23–2.72 Å (average 2.51 Å). Nine dipole-dipole interactions, eighteen of ion-dipole interactions, and ten interactions to perchlorates contribute to the crystal packing of complex **6**, [Cu(**3**)MeCN]·$2ClO_4$ (Fig. 11).

In all the metallated structures, **4** – **6**, the complexes exist in the crystalline state with some degree of propellar-like twist of the three pyridyl-based ligands. One helical twist over another will dominate when a chiral ligand is bound in solution, thereby giving rise to a Cotton effect in the circular dichroism spectra.[28] In the lack of a chiral ligands, the helical twists would be rapidly interconverting, a phenomenon that cannot occur in the solid state.

Conclusions

We have synthesized and characterized a set of three TPMA-based ligands and a set of their copper(II) complexes, in which the number of phenylethynyl substituents at the 6-position of the pyridyl ring was varied. We present here an extensive study of the intermolecular interactions found in the solid state. Crystal structures of the series of compounds reveal expected triangular geometries for free ligands and propeller-like structures for their copper complexes. Examination of short contacts among the molecules in solid-state of **1**–**6** shows seventy non-covalent interactions including [C–H···N], [C–H···π], and [π···π] contacts. Identified hydrogen bonds are in the boundary of a weak interaction with 3.2–4.0 Å of the donor-acceptor distance. The phenylethynyl substituent provides a variety of [C–H···π] contacts, and plays a key role in all of six crystal structures. Surprisingly, the most basic nitrogen in free ligand **1**–**3**, the tertiary amine nitrogen, does not form any short contacts to its neighbouring molecules due to sterics from the

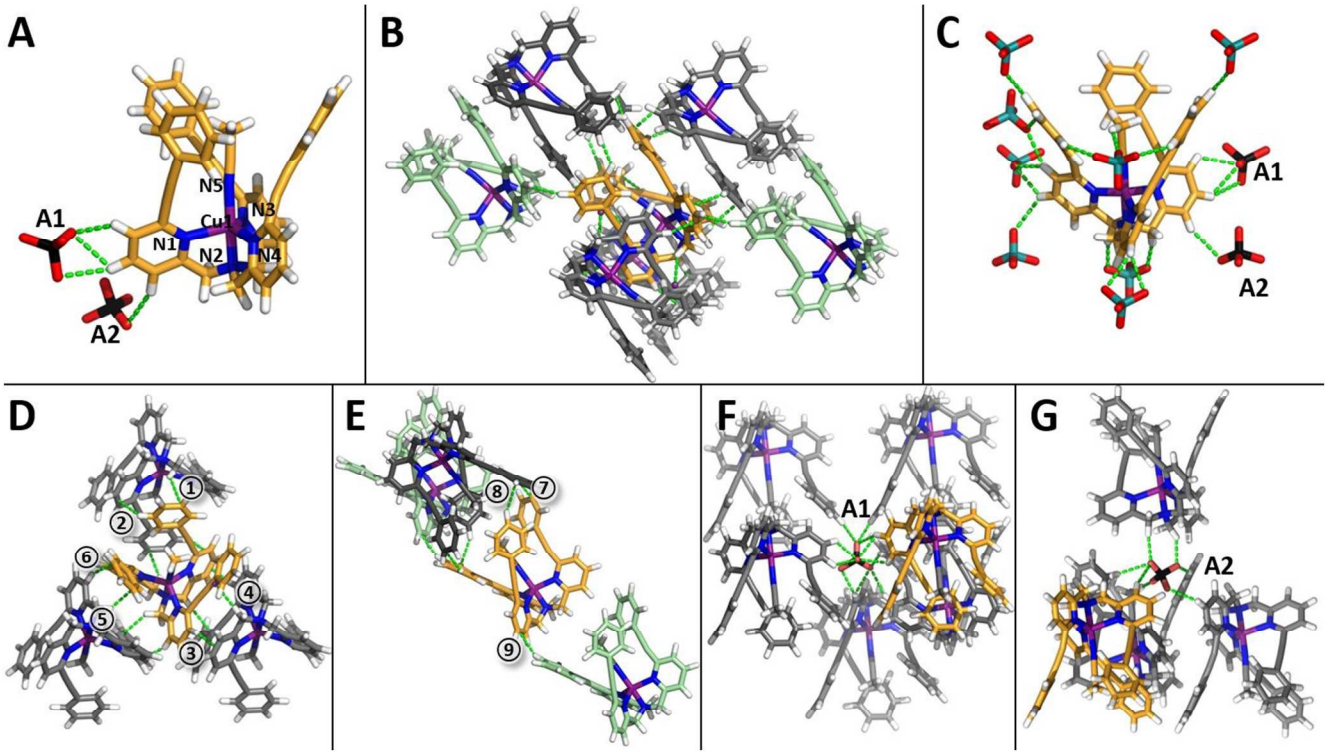

Fig. 10 (A) Crystal structure of the asymmetric unit of compound **6** [Cu(**3**) MeCN]·$2ClO_4$. (B) Intermolecular short contacts of the cationic Cu^{2+} complex **6** with three other Cu^{2+} complexes, and the details (D) and (E). *Contact 1*: type *xi*, C–H···C 2.84 Å, C···C 3.68 Å, ∠C–H···C 4.3°. *Contact 2*: type *iv*, C–H···C=$C_{centroid}$ 2.75 Å, C···C=$C_{centroid}$ 3.49 Å, ∠C–H···C=$C_{centroid}$ 125.1°. *Contact 3*: type *iv*, C–H···C=$C_{centroid}$ 2.34 Å, C···C=$C_{centroid}$ 3.38 Å, ∠C–H···C=$C_{centroid}$ 159.6°. *Contact 4*: type *xii*, C–H···C=C–$C_{centroid}$ 2.51 Å, C···C=C–$C_{centroid}$ 3.41 Å, ∠C–H···C=C–$C_{centroid}$ 140.2°. *Contact 5*: type *xi*, C–H···C 2.72 Å, C···C 3.52 Å, ∠C–H···C 130.0°. *Contact 6*: type *v*, C–H···C 2.65 Å, C···C 3.67 Å, ∠C–H···C 157.1°. *Contact 7*: type *v*, C–H···C 2.90 Å, C···C 3.68 Å, ∠C–H···C 128.8°. *Contact 8*: type *v*, C–H···C 2.78 Å, C···C 3.79 Å, ∠C–H···C 154.3°. *Contact 9*: type *v*, C–H···C 2.84 Å, C···C 3.87 Å, ∠C–H···C 156.7°. (C) Eighteen short contacts of cationic Cu^{2+} complex with ten of perchlorate anions. (F) Eleven short contacts of anion A1 with six of cationic Cu^{2+} complexes, and (G) Seven short contacts of anion A2 with four of cationic Cu^{2+} complexes. C—orange, pale green, dark gray and gray, H—white, N—blue, O—red, Cl—black and deep teal, Cu—deep purple, and centroid—violet purple.

partially positive hydrogens on the pyridyl rings.

Our future work in this area is aimed at the development of optical sensors for enantiomeric excess measurement in liquid- and solid-state based on the binding properties of TPMA to metal ions. We believe that this preliminary study will inform these and relevant studies of this intriguing class of TPMA derivatives.

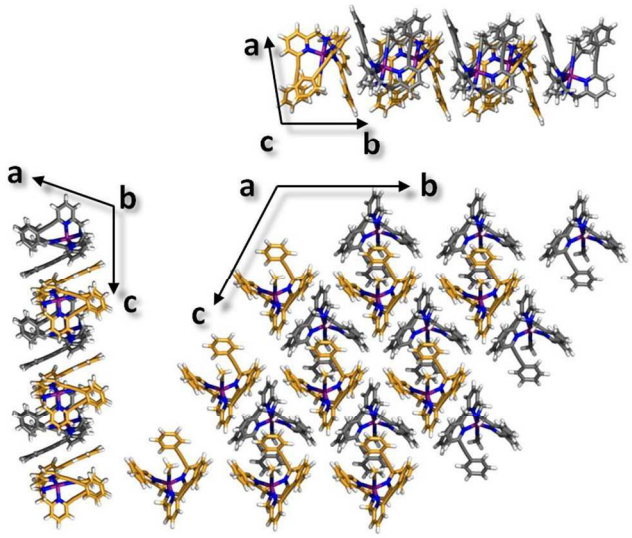

Fig. 11 Partial crystal packing ($a \times b \times c$ = 1×3×3) viewed from three axes for compound **6**. Molecules in the same color face the same direction, and perchlorates are omitted. C—orange and gray, H—white, N—blue, and Cu—deep purple.

Acknowledgements

The authors gratefully acknowledge the financial support from the National Science Foundation (CHE-1212971), and the Welch Foundation (F-0046).

Notes and references

[a] Department of Chemistry, The University of Texas at Austin, Austin, Texas, USA 78752. E-mail: anslyn@austin.utexas.edu

[b] Institute for Cellular and Molecular Biology, The University of Texas at Austin, Austin, Texas, USA 78752. E-mail:ellingtonlab@gmail.com

† Electronic Supplementary Information (ESI) available: NMR and crystallographic information. CCDC 1028485–1028490. For ESI and crystallographic data in CIF or other electronic format see DOI: 10.1039/b000000x/

1 C. E. Tornow, M. R. Thorson, S. Ma, A. A. Gewirth and P. J. A. Kenis, *J. Am. Chem. Soc.*, 2012, **134**, 19520.

2 H. Sugimoto, K. Kitayama, S. Mori and S. Itoh, *J. Am. Chem. Soc.*, 2012, **134**, 19270.

3 A. L. Ward, L. Elbaz, J. B. Kerr and J. Arnold, *Inorg. Chem.*, 2012, **51**, 4694.

4 T. Kojima, K. Nakayama, K. Ikemura, T. Ogura and S. Fukuzumi, *J. Am. Chem. Soc.*, 2011, **133**, 11692.

5 D. G. Lonnon, D. C. Craig and S. B. Colbran, *Dalton Trans.*, 2006, 3785.

6 M. Krom, T. P. J. Peters, R. G. E. Coumans, T. J. J. Sciarone, J. Hoogboom, S. I. t. Beek, P. P. J. Schlebos, J. M. M. Smits, R. d. Gelder and A. W. Gal, *Eur. J. Inorg. Chem.*, 2003, 1072.

7 A. Hazell, J. McGinley and H. Toftlund, *Inorg. Chim. Acta*, 2001, **323**, 113.

8 C. S. Allen, C. –L. Chuang, M. Cornebise and J. W. Canary, *Inorg. Chim. Acta*, 1995, **239**, 29.

9 L. Natrajan, J. Pécaut, M. Mazzanti and C. LeBrun, *Inorg. Chem.*, 2005, **44**, 4756.

10 K. Ishimori, M. Watanabe, T. Kimura, T. Yaita, T. Yamada, Y. Kataoka, S. Shinoda and H. Tsukube, *Chem. Lett.*, 2005, **34**, 1112.

11 F. Bravard, C. Rosset and P. Delangle, *Dalton Trans.*, 2004, 2012.

12 L. Karmazin, M. Mazzanti and J. Pécaut, *Inorg. Chem.*, 2003, **42**, 5900.

13 R. Wietzke, M. Mazzanti, J. –M. Latour, J. Pécau, P. –Y. Cordier and C. Madic, *Inorg. Chem.*, 1998, **37**, 6690.

14 A. Hazell, J. McGinley and H. Toftlund, *J. Chem. Soc., Dalton Trans.*, 1999, 1271.

15 C. -L. Chuang, M. Frid and J. W. Canary, *Tetrahedron Lett.*, 1995, **36**, 2909.

16 S. K. Brownstein, P. -Y. Plouffe, C. Bensimon and J. Tse, *Inorg. Chem.*, 1994, **33**, 354.

17 M. R. Bukowski, P. Comba, A. Lienke, C. Limberg, C. L. d. Laorden, R. Mas-Ballesté, M. Merz and L. Que, Jr., *Angew. Chem. Int. Ed.*, 2006, **45**, 3446.

18 R. Mas-Ballesté and L. Que, Jr., *J. Am. Chem. Soc.*, 2007, **129**, 15964.

19 V. O. Rodionov, S. I. Presolski, D. D. Díaz, V. V. Fokin and M. G. Finn, *J. Am. Chem. Soc.*, 2007, **129**, 12705.

20 A. J. Clark, *Chem. Soc. Rev.*, 2002, **31**, 1.

21 T. Pintauer and K. Matyjaszewski, *Chem. Soc. Rev.*, 2008, **37**, 1087.

22 S. Zahn and J. W. Canary, *J. Am. Chem. Soc.*, 2002, **124**, 9204.

23 S. Zahn, G. Proni, G. P. Spada and J. W. Canary, *Chem. Eur. J.*, 2001, 7, 88.

24 S. Zahn and J. W. Canary, *Science*, 2000, **288**, 1404.

25 S. Zahn and J. W. Canary, *Org. Lett.*, 1999, **1**, 861.

26 J. W. Canary, C. S. Allen, J. M. Castagnetto, Y. –H. Chiu, P. J. Toscano and Y. Wang, *Inorg. Chem.*, 1998, **37**, 6255.

27 J. W. Canary, C. S. Allen, J. M. Castagnetto and Y. Wang, *J. Am. Chem. Soc.*, 1995, **117**, 8484.

28 L. A. Joyce, M. S. Maynor, J. M. Dragna, G. M. d. Cruz, V. M. Lynch, J. W. Canary and E. V. Anslyn, *J. Am. Chem. Soc.*, 2011, **133**, 13746.

29 T. Zhang, N. Y. Edwards, M. Bonizzoni and E. V. Anslyn, *J. Am. Chem. Soc.*, 2009, **131**, 11976.

30 H. H. Jo, R. Edupuganti, L. You, K. N. Dalby and E. V. Anslyn, *Chem. Sci.*, 2015, **6**, 158.

31 H. H. Jo, C. –Y. Lin and E. V. Anslyn, *Acc. Chem. Res.*, 2014, **47**, 2212.

32 L. You, J. S. Berman, A. Lucksanawichien and E. V. Anslyn, *J. Am. Chem. Soc.*, 2012, **134**, 7126.

33 L. You, G. Pescitelli, E. V. Anslyn and L. D. Bari, *J. Am. Chem. Soc.*, 2012, **134**, 7117.

34 L. You, S. R. Long, V. M. Lynch and E. V. Anslyn, *Chem. Eur. J.*, 2011, **17**, 11017.

35 L. You, J. S. Berman and E. V. Anslyn, *Nat. Chem.*, 2011, **3**, 943.

36 T. Zhang, N. Y. Edwards, M. Bonizzoni and E. V. Anslyn, *J. Am. Chem. Soc.*, 2009, **131**, 11976.
37 S. L. Tobey and E. V. Anslyn, *Org. Lett.*, 2003, **5**, 2029.
38 S. L. Tobey, B. D. Jones and E. V. Anslyn, *J. Am. Chem. Soc.*, 2003, **125**, 4026.
39 H. H. Tsukube, J. Uenishi, H. Higaki, K. Kikkawa, T. Tanaka, S. Wakabayashi and S. Oae, *J. Org. Chem.*, 1993, **58**, 4389.
40 R. F. Heck, *Palladium Reagents in Organic Synthesis*; Academic Press: London/Orlando, 1985, pp. 18.
41 S. Abada, A. Leconitre, M. Elhabiri and L. J. Charbonnière, *Dalton Trans.*, 2010, **39**, 9055.
42 G. Pelletier and A. B. Charette, *Org. Lett.*, 2013, **15**, 2290.
43 N. Wei, N. N. Murthy, Q. Chen, J. Zubieta and K. D. Karlin, *Inorg. Chem.*, 1994, **33**, 1953.
44 J. W. Canary, A. E. Holmes and J. Liu, *Enantiomer*, 2001, **6**, 181.
45 G. A. Jeffrey, *An Introduction to Hydrogen Bonding*, Oxford University Press, Oxford, 1997, pp 12.